# Early Monitoring of Forest Wood-Boring Pests with Remote Sensing

Youqing Luo, Huaguo Huang, Alain Roques

ANNUAL REVIEWS

*Annual Review of Entomology*

# Early Monitoring of Forest Wood-Boring Pests with Remote Sensing

Youqing Luo,[1,2,*] Huaguo Huang,[3] and Alain Roques[2,4]

[1]Beijing Key Laboratory for Forest Pest Control, Beijing Forestry University, Beijing, P.R. China; email: yqluo@bjfu.edu.cn

[2]Sino-French Joint Laboratory for Invasive Forest Pests in Eurasia, Beijing Forestry University/French National Research Institute for Agriculture, Food and Environment (INRAE), Beijing, P.R. China/Paris, France

[3]Research Center of Forest Management Engineering of State Forestry and Grassland Administration, Beijing Forestry University, Beijing, P.R. China; email: huaguo_huang@bjfu.edu.cn

[4]INRAE—Zoologie Forestière, Centre de recherche Val de Loire, Orléans, France; email: alain.roques@inra.fr



Annu. Rev. Entomol. 2023. 68:277–98

First published as a Review in Advance on October 5, 2022

The *Annual Review of Entomology* is online at ento.annualreviews.org

https://doi.org/10.1146/annurev-ento-120220-125410



*Corresponding author

## Keywords

forest insects, wood-boring pests, remote sensing, early detection, unmanned aerial vehicle, UAV, satellite

## Abstract

Wood-boring pests (WBPs) pose an enormous threat to global forest ecosystems because their early stage infestations show no visible symptoms and can result in rapid and widespread infestations at later stages, leading to large-scale tree death. Therefore, early-stage WBP detection is crucial for prompt management response. Early detection of WBPs requires advanced and effective methods like remote sensing. This review summarizes the applications of various remote sensing sensors, platforms, and detection methods for monitoring WBP infestations. The current capabilities, gaps in capabilities, and future potential for the accurate and rapid detection of WBPs are highlighted.

## 1. INTRODUCTION

**Remote sensing (RS):** techniques to detect radiation and reflection, emission, or scattering characteristics without coming in contact with the observed objects

**UAV:** unmanned aerial vehicle

**Hyperspectral:** imaging technology that uses many narrow wavebands (usually <10 nm wide) to analyze object composition

**Light detection and ranging (LiDAR):** method using laser beams to measure the 3D position, intensity, and waveform of objects

**Radio detection and ranging (radar):** system for transmitting and receiving radio waves to detect the scattering characteristics of objects

Pests and diseases cause considerable damage to forest ecosystems globally. Among them, insect damage is predominant (26). According to 2009 Food and Agriculture Organization (FAO) statistics, Coleopterans account for the vast majority of insect damage to forests (26). Coleopterans include wood-boring pests (WBPs) such as *Ips typographus*, *Dendroctonus ponderosae*, *Dendroctonus rufipennis*, *Anoplophora glabripennis*, *Anoplophora chinensis*, and *Agrilus planipennis*. Generally, WBP larvae or adults burrow under the trunk xylem or phloem and bore dense tunnels, blocking the transportation of plants' nutrients and water, leading to the withering and death of the infested trees (91). In contrast to the obvious symptoms noticed in the case of the defoliators, WBPs have a hidden lifestyle, and their presence results in delayed symptoms. Infested trees show obvious damage signs only in the middle and late stages of infestation, making the detection and control of the pests challenging. In addition, the damage caused by WBPs to a tree's transport tissue is irreversible, unlike the damage caused by defoliators, which can be recovered by the growth of new leaves during the next growing season. WBP damage spreads to large areas quickly. Therefore, there is an urgent need for monitoring and warning tools for WBP damage early in the infestation cycle. While traditional ground surveys can be used at small scales, remote sensing (RS) technology can be a good choice for large-scale monitoring.

RS technology provides a powerful tool to monitor different stages of pest disturbance at large scales, continuously, and in a timely manner. This technology, combined with expert diagnosis, can help objectively assess infestation damage and accurately predict its occurrence, thereby providing a scientific basis for appropriate forest management. Related research can be traced back to the 1930s, when aerial photography was used to observe deciduous forests damaged by *Lambdina fiscellaria* (58). Since the 1980s, the number of RS monitoring studies of WBPs has been increasing (6, 51, 100).

Monitoring WBPs in the early stages of infestation (i.e., identifying infested trees before they show obvious symptoms) is challenging and has required RS technology advances. In recent decades, remarkable progress in satellites' temporal, spatial, and spectral resolutions has led to increased availability of multiscale, multitemporal, and multisource RS data. Flexible unmanned aerial vehicles (UAVs), combined with new lightweight sensors like hyperspectral imagers, light detection and ranging (LiDAR), radio detection and ranging (radar), and thermal cameras, provide multidimensional, convenient, and high-quality data that can support the early monitoring of WBPs.

The monitoring or assessment of forest health (including insect pests) using RS technology has been reviewed previously (73, 106, 107, 114). However, there is no comprehensive review on WBP early monitoring with RS. In this article, we review studies of state-of-the-art RS technology applied to the early monitoring of WBPs at different scales, using various sensors and monitoring models, and identify some problems and prospects. The present review focuses on several globally important forest WBPs, including species endangering conifers, such as *Monochamus* spp. spreading *Bursaphelenchus xylophilus*, *I. typographus*, *D. ponderosae*, *D. rufipennis*, *D. valens*, *Tomicus* spp., and *Sirex noctilio*, and species damaging broad-leaved trees, including *A. planipennis* and *A. glabripennis*.

We first discuss what is known about the biology and ecology of coleopteran tree pests, then discuss different RS technologies. We follow this discussion with a systematic review of how different RS technologies have been used to monitor insect pests and critically evaluate the different approaches. Finally, key issues and technologies are proposed for future consideration.

## 2. BIOLOGY AND ECOLOGY

Following a WBP attack on a tree, water or nutrient transport may be blocked, impacting the physiology of leaves (such as chlorophyll content, water content, photosynthesis, and

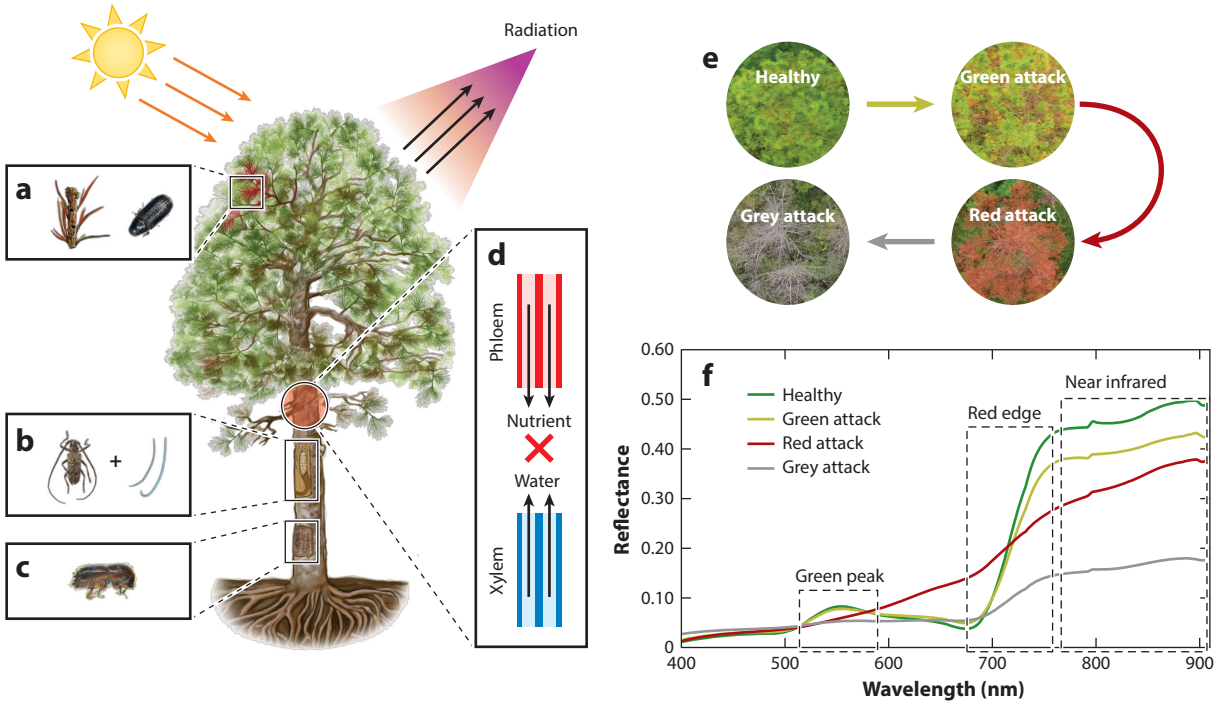


**Figure 1**

Schematics of the remote sensing signal responses to the biological and morphological changes caused by wood-boring pests (WBPs) (not limited to the species shown in panels *a–c*). (*a*) *Tomicus* spp. damage shoots and trunks. (*b*) The company *Monochamus* spp.–*Bursaphelenchus xylophilus* damage trunks and branches. (*c*) *Ips typographus* damage trunks. (*d*) Xylem or phloem damaged by WBPs, disrupting water and nutrient transportation. (*e*) Three significant infestation stages on a tree crown. (*f*) Hyperspectral curves for the various stages of infestation shown in panel *e*.

transpiration). This leads to progressive changes in the appearance of the tree (such as leaf discoloration) and possibly indicates a typical infestation stage (2, 13, 72, 131) (**Figure 1**). There are very few early monitoring studies of WBPs involving broad-leaved trees. Therefore, we take as an example the well-studied infestation stage classification of WBPs damaging coniferous trees, specifically *I. typographus* and *D. ponderosae*. The damage caused by WBPs can be classified into three stages: green attack, red attack, and gray attack. In the green attack stage, needles and crowns remain green even though their physiology starts to change. In the red attack stage, the trees become dehydrated, the structure of leaf cells and tissues gets destroyed, chlorophyll gets decomposed, and the leaf color gradually changes from green to yellow and red. Finally, in the gray attack stage, the trees lose water completely and wither, causing all the tree needles to fall off, leaving a gray crown (2, 16, 27, 124). These symptoms of a WBP infestation can cause changes in the spectral and structural information available about tree leaves and canopy, which provide the basis for RS-based monitoring of WBPs at the early stage. For example, the red edge band (680–760 nm) shifts to shorter wavelengths in stressed trees compared with healthy trees (27, 72, 131) (**Figure 1*f***).

**Red edge:** spectral region where vegetation reflectance changes rapidly between the red and NIR portions of the electromagnetic spectrum

WBPs generally spread from a single tree to a large area. Removing single infested trees at the early stages can quickly restrain the spread. Previous studies mainly focused on monitoring the red or gray attack stages (15, 20, 31, 38, 77, 78, 121). At these stages, WBPs have usually already spread widely, and it is costly and ineffective to remove red or gray trees. Therefore, RS

**Table 1 Remote sensors commonly used in WBP early detection**

| Sensors | Advantages | Shortcomings | Feature parameters |
|---|---|---|---|
| Visible-light camera | Low cost, high mobility, and high spatial resolution | Three bands with limited spectral information | RGB image, texture and spatial information |
| Multispectral sensor | Low cost, red edge or near infrared bands included | Wide bands with low spectral resolution, from 4 to approximately 10 bands | Multispectral image, multichannel reflectance |
| Hyperspectral sensor | Rich spectral information, hundreds of narrow-band reflectances | High cost, huge data volume, complex data processing | Hyperspectral data cube, texture and spatial information |
| Thermal imager | Acquisition of canopy temperature and emissivity | Coarse resolution, rapid temperature variation, uncertainty of atmospheric correction | Thermal infrared image, temperature, and emissivity |
| LiDAR | Direct 3D measurement of trees, high canopy penetration | High cost, only one to two wavelengths, limited and discrete footprint | Point cloud, waveform, and canopy height model |
| Radar | All weather; certain canopy penetration; sensitive to biomass, water, and deformation | High speckle noise, complex imaging geometry, limited frequencies | Radar image, polarimetric scattering, and interferometry |

Abbreviations: LiDAR, light detection and ranging; radar, radio detection and ranging; RGB, red, green, and blue; WBP, wood-boring pest.

technology should aim for early monitoring of WBPs to reduce losses, which is the primary goal of forest managers and a current important research topic (3, 8, 33, 47, 52, 57, 59, 126, 128–131).

## 3. MONITORING SCALES AND SENSORS

There are generally four kinds of RS platforms that can be used to monitor WBP damage, including ground instruments to monitor needles, UAVs for stand evaluations, manned aircraft for ecosystem-wide observations, and even satellites for landscape- or global-scale analysis. These platforms can be used for different scales of monitoring generally considered in the literature. Ground-scale studies reveal the relationship between the physiological and biochemical characteristics of needles and RS information (such as spectral reflectance), providing a theoretical basis for larger-scale monitoring. Airborne-scale studies (using UAVs or manned aircrafts) bridge the ground and satellite scales. Satellites provide the only practical way to achieve regional-scale or global monitoring of WBPs. Therefore, early monitoring of WBPs is scale dependent, and the monitoring objectives, scope, and effects at different scales are complementary.

Advancements in sensors, such as visible-light cameras, multispectral or hyperspectral imagers (HI), thermal infrared (TIR) imagers, LiDAR, and radar equip RS technologies with many tools for WBP early monitoring via collecting diverse information at different scales (**Table 1**). Through data transmission, conversion, and processing, quantitative interpretations of tree health status have been made (73). Multisensor data fusion, such as the LiDAR-HI fusion (70, 130) and LiDAR-TIR-HI fusion (95), can combine observations from two or more sensors to provide more robust or accurate WBP damage detection.

**Visible:** electromagnetic spectrum range from 400 nm to 700 nm

**Thermal infrared (TIR):** RS that uses TIR radiation information to determine the surface temperature radiated by objects in the spectral range of 8–14 μm

## 4. SYSTEMATIC REVIEW

We examined 1,736 research articles published between 2005 and 2021 on the Web of Science using “insects/pests” and “remote sensing/remotely sensed” as keywords. **Figure 2** shows the

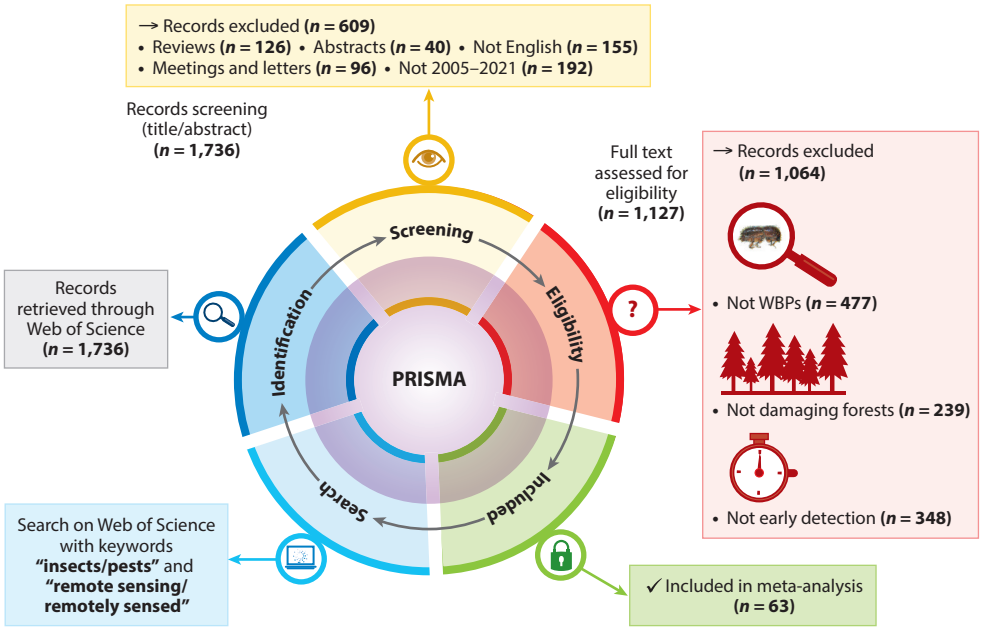


**Figure 2**

PRISMA flow diagram of study inclusion and exclusion. Abbreviations: PRISMA, Preferred Reporting Items for Systematic Review and Network Meta-analysis; WBP, wood-boring pest.

search process and inclusion and exclusion criteria following the Preferred Reporting Items for Systematic Review and Network Meta-analysis (PRISMA) standards for systematic reviews. Of the articles examined, 63 covered the early monitoring of WBPs using RS technology, among which more than half ($n = 35$) were published only recently (2017–2021), indicating that increased attention is being paid to the early monitoring of WBPs.

Noticeably, the research on WBPs endangering conifers was more extensive and in-depth (accounting for 90% of the studies) than the research on broad-leaved trees. The most-studied WBP species are *I. typographus*, *D. ponderosae* and the company *Monochamus* spp.–*B. xylophilus*; however, there are relatively few early monitoring studies on other WBPs, such as *S. noctilio* (**Figure 3**). The studies are also unevenly distributed globally: More are located in North America ($n = 23$), East Asia ($n = 20$), central and northern Europe ($n = 18$) and South Africa ($n = 2$) than in other regions. This disparity may indicate less access to RS technologies or insufficient research budgets in these other regions.

With respect to the scale of analysis, nearly two-thirds of the studies are based on airborne data. In terms of sensors, hyperspectral data are the most widely used in WBP early monitoring, followed by LiDAR (**Figure 4**). For WBP species, there is no clear rule for selecting an optimal or specified sensor or platform. Additionally, RS signal responses to damage on coniferous or broad-leaved trees is consistent for both native species and invaders. Therefore, we prefer to discuss the state-of-the-art research and applications in WBP early monitoring from the technology viewpoint, rather than from the perspective of pests or host tree species.

We comment separately on the key issues of satellite RS monitoring because satellite platforms used in this field have varying spatial scales, from submeter to 30 m; comprehensive space coverage; multiple spectral bands; and periodic revisit intervals, all of which are unique compared with airborne-scale monitoring.

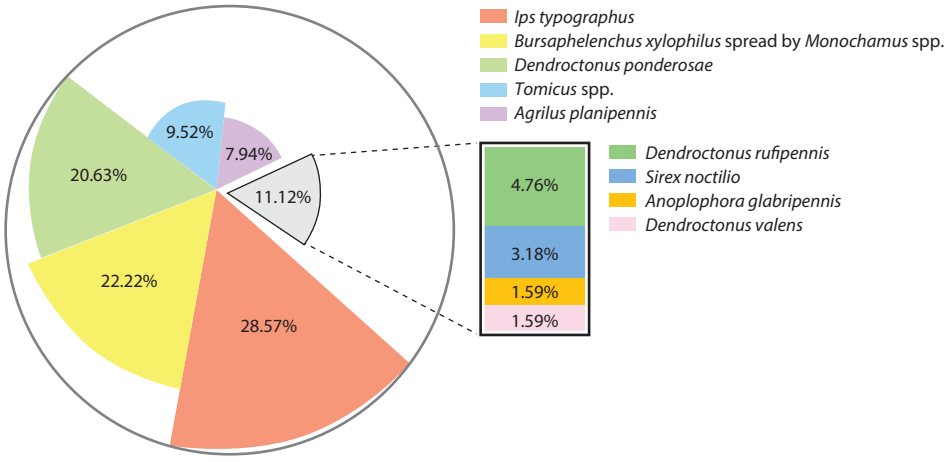


**Figure 3**

Number of early monitoring studies on different wood-boring pest species.

## 4.1. Unmanned Aerial Vehicle Visible-Light and Multispectral Remote Sensing

**RGB:** red, green, and blue

Visible light refers to a small portion (400–780 nm) of the electromagnetic spectrum that can be perceived by human eyes, remotely sensed mainly with red, green, and blue (RGB) bands. With the recent development of ground-based RS and UAVs, visible light data have been used in WBP monitoring (61, 122, 125, 134). UAVs mounted with visible-light cameras can rapidly collect high-resolution images of forest canopies with low cost, high flexibility, and low requirements for clear sky conditions. Therefore, they are mainly used to detect damaged trees by applying deep learning models (122, 125, 134). However, the detection accuracy is not satisfying if one is only using visible-light data at the early stage of WBP infestation. Early detection of *B. xylophilus* using visible-light data had an accuracy of only 0.465–0.508 (122). There are two reasons for this low performance: (*a*) The spectral information is insufficient, and (*b*) most studies focus on identifying trees with obvious discoloration (115, 125, 134) instead of early stage detection.

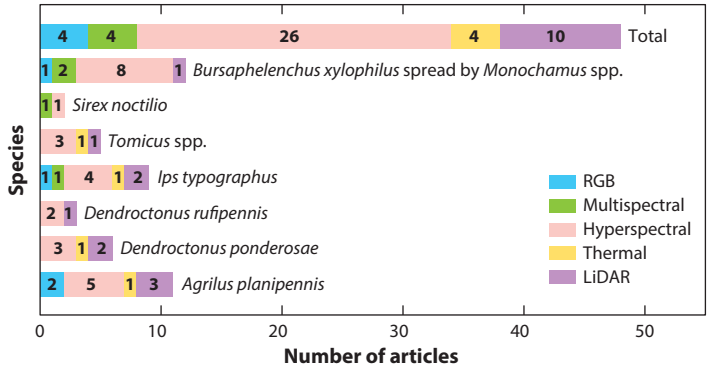


**Figure 4**

Number of studies using different remote sensing sensors in wood-boring pest early monitoring. Abbreviations: LiDAR, light detection and ranging; RGB, red, green, and blue.

In addition to RGB, multispectral data used for WPB monitoring also include near-infrared (NIR) bands and, more recently, red edge bands (56, 77, 98, 129). Among these studies, there are few on early detection. To detect *B. xylophilus*, UAV-based multispectral data were used to identify pine trees with early stage damage, but the results were not promising (56, 129). Despite the usefulness of NIR or red edge bands, the bandwidth of multispectral bands is still too wide to be successfully applied for early monitoring.

In general, visible-light and multispectral RS are limited by spectral resolution and thus are only suitable for monitoring discolored trees in the middle or late stages.

**Near-infrared (NIR):** electromagnetic spectrum range from 700 nm to 1,000 nm

**Shortwave infrared region (SWIR):** electromagnetic spectrum range from 1,000 nm to 2,500 nm

## 4.2. Hyperspectral Remote Sensing from Different Platforms

Hyperspectral RS collects data from hundreds of bands and continuous wavelengths from visible light to NIR (400–1,000 nm) and shortwave infrared region (SWIR) (1,000–2,500 nm). These bands can capture physiological changes in infested trees, which helps in detecting WPB infestations at the early stages (2, 13, 72, 131).

Ground-based hyperspectral RS is routinely performed for WBP monitoring and is essential for feature screening and model verification. It also provides a priori knowledge to build spectral libraries or identify the most sensitive bands for larger-scale monitoring (2, 13, 24, 31, 33, 71, 72, 131). A study transferred the sensitive SWIR bands identified from ground-based hyperspectral curves to satellite images and successfully detected the early stage of a bark beetle infestation (33). Similarly, optimized indices such as red edge parameters from ground-based hyperspectral data produced the highest accuracy in UAV-based hyperspectral data for *B. xylophilus* early monitoring (131). However, ground-based hyperspectral data usually consist of a few spectral curves of limited samples with no imaging capability; thus, their application to a large area or a large number of data acquisitions is time consuming and laborious, making their use challenging (131, 140). To increase the observation area, a tower-based spectroradiometer was used to analyze the interaction between pine canopy reflectance and bark beetle stress at different infestation stages (45), but the scope was still limited.

As the primary technology used in WBP early monitoring (**Figure 4**), airborne (including UAV-based) hyperspectral imagery can provide highly accurate detection with flexible and efficient data acquisition (27, 56, 66, 67, 69, 70, 113, 137). Most studies used single-date airborne hyperspectral data for early monitoring of WBPs (27, 66, 70, 95, 96, 128, 130, 131). The use of time-series data is relatively rare (13, 24, 56, 72, 113), even though it could be used to capture relatively complete infestation processes, thus leading to more reliable results than those based on a single date, with the limitation that any changes observed in the color and texture of tree crowns could also be due to phenology and other factors.

With the expansion of the study area, the number of bands and images to be scanned in airborne hyperspectral data acquisition increases, raising the cost and complexity of image processing and also requiring geographic registration and image stitching (e.g., combining overlapped images to create a panoramic image). Satellite sensors can be used to obtain images from a large area and therefore can be applied to large-scale WBP early monitoring. However, suitable spaceborne hyperspectral data are not yet operationally available. The Moderate-Resolution Imaging Spectrometer (MODIS) has tens of spectral bands, but its spatial resolution is too low (250–1,000 m). Hyperion and the Compact High Resolution Imaging Spectrometer (CHRIS) have more bands and higher spatial resolution than MODIS, but they have been retired, and their image widths are only 7.7 km and 14.0 km, respectively. Despite their great potential for WBP early monitoring, China's Orbita Hyperspectral (OHS) satellite, with a spatial resolution of 10 m, a swath width of 150 km, and 256 bands (400–1,000 nm), and Gaofen-5, with a spatial resolution of 30 m, a swath width of 60 km, and 330 bands (400–2,500 nm), are not yet operationally available

and have not yet been applied to specific monitoring efforts, but they should be evaluated in future research.

**Sun-induced chlorophyll fluorescence (SIF):** a small light signal emitted from green plants during photosynthesis

Furthermore, sun-induced chlorophyll fluorescence (SIF) (81, 82, 84) may also be applied to WBP early monitoring. Compared with traditional monitoring methods based on greenness vegetation indices, chlorophyll fluorescence, which has been widely used in crop stress monitoring, directly relates to leaf photosynthesis and responds quickly to stress (111, 132). However, there is almost no research using SIF to detect WBPs.

In summary, hyperspectral RS can capture even the slightest changes in physiological characteristics of trees before the appearance of obvious symptoms, suggesting a potential role in the early monitoring of WBPs. As for band selection, NIR is generally involved in most studies, although the red edge and SWIR are the most sensitive for WBP early monitoring, as demonstrated by the frequency with which they are used in the literature. However, the insufficient satellite data sources, large amounts of data, complex data analysis, and high costs associated with these bands are problems that still need to be addressed.

## 4.3. Thermal Remote Sensing from Different Platforms

TIR RS collects thermal emissions from the land surface and transforms them into digital temperature images. Temperature, to some degree, is indicative of the canopy energy balance and is sensitive to changes in water deficit, leaf transpiration intensity, and photosynthetic rate (10). Thus, TIR technology has been widely used to monitor vegetation water deficit and pest or disease stress symptoms (103, 109).

However, few studies on WBP early monitoring make use of TIR technology (3, 75, 95, 108, 120). Ground-based thermal imaging has been used to identify trees damaged by bark beetles at an early stage, confirming the significant correlation between temperature and damage degree of trees (75, 120). An airborne TIR camera was combined with hyperspectral and LiDAR sensors to successfully map the distribution of ash trees, providing a novel approach for early monitoring of *A. planipennis* (95). The green attack stage of *I. typographus* has been detected using both the optical and TIR data of Landsat 8. The inversed canopy surface temperature outperformed the spectral vegetation indices in monitoring slight changes caused by insect damage (3).

In the early stage of a WBP infestation, trees still have a certain capacity to adjust their physiological and biochemical parameters to survive. Consequently, negligible changes in canopy structural and spectral information are too difficult to detect by optical sensors. Since TIR is sensitive to water content variations, it may be better suited to detect damaged trees at an early stage (108, 120). However, TIR data collection is limited to clear-sky conditions. In addition, the image resolution of TIR is significantly coarser than that of optical images; thus, the mixed-pixel issues need to be addressed before TIR can be more widely applied (142). Factors like drought also cause abnormal changes in surface temperature, and TIR may not accurately distinguish different pests, diseases, and abiotic stress-induced changes (120).

The temporal or spatial resolution of the TIR band of the most widely used satellites is insufficient to satisfy the requirements for early monitoring. Landsat 8 has a TIR band with a spatial resolution of 100 m, but the temporal resolution is 16 days or even longer due to clouds and rain. Few spaceborne TIR sensors have a high temporal and spatial resolution. China's Gaofen-5 has a spatial resolution of 40 m in the TIR band, suitable for monitoring temperature anomalies at a plot scale. The NASA Ecosystem Spaceborne Thermal Radiometer Experiment on Space Station (ECOSTRESS) is another potential tool and has a pixel size of approximately 38 m × 69 m and a revisit period of 1–5 days (32).

Despite the above limitations, the potential of TIR technology for WBP early monitoring needs to be further investigated.

## 4.4. Active Remote Sensing: LiDAR and Radar Sensors

Passive optical RS provides two-dimensional images under clear-sky conditions. By directly measuring the 3D structure information of objects, LiDAR is sensitive to structural changes and has been widely used in forest health assessments (62, 90, 135), including detection of defoliators (53, 54, 80, 110) and WBPs (16, 50, 59, 69, 70, 95, 112, 113, 130).

**Synthetic aperture radar (SAR):** an active radar system providing high-spatial-resolution all-weather surface penetration ability

Microwave radar has a high penetration ability, which helps it obtain useful data on cloudy and rainy days. Because radar backscattering or interference data contain information related to forest pests and diseases, they have also been used in WBP monitoring in recent years (52, 93).

LiDAR and radar have been used at different scales. Two ground LiDAR systems with 905 nm and 1,550 nm wavelengths, respectively, were used to detect the early stage of *I. typographus* with an overall accuracy of 62–67% (59). By combining UAV-based LiDAR with hyperspectral data, researchers have monitored *Tomicus* spp. and *B. xylophilus* with a higher accuracy than by using hyperspectral sensing alone (70, 130). Airborne LiDAR also improved the classification accuracy of host tree species damaged by *A. planipennis* (95). At the spaceborne scale, the L-band synthetic aperture radar (SAR) was used to detect forests damaged by *I. typographus*, confirming the efficiency of backscatter data for outbreak detection but with a low early monitoring accuracy (64–74%). Combining TerraSAR-X radar and RapidEye multispectral data resulted in an early monitoring accuracy of 74% for *I. typographus* infestation compared to 23% using radar data alone (93). Recent monitoring of the early stage of *I. typographus* using time series backscatter data from Sentinel-1 was not convincing (52).

Unlike defoliators, which cause evident morphological changes in trees, WBPs generally cause systematic damage, with almost no defoliation in the early stages. Therefore, LiDAR alone is not expected to be an optimal choice for WBP early monitoring (130).

In future research, the following suggestions need to be carefully considered for the early detection of WBPs. LiDAR systems should be upgraded to have a smaller sampling interval and footprints comparable to single shoots or needles to obtain detailed structural information for more accurate detection (50). Moreover, multiwavelength LiDAR systems are needed. Most studies used single-wavelength LiDAR sensors, at either 905 nm (50, 59, 69, 70, 130) or 1,550 nm (95, 112, 113), which did not fully exploit the intensity information. Multisource data fusion is highly recommended. The use of LiDAR or radar data alone for WBP early monitoring resulted in low accuracy (52, 93, 116, 130). In contrast, fusing LiDAR or radar data with optical RS or TIR data produced a higher accuracy (70, 93, 95, 130).

## 4.5. Resolution of Satellite Remote Sensing

**Table 2** shows the nine main types of satellite sensors used for WBP early monitoring, with different spatial, spectral, and temporal resolutions. Except for Sentinel-1 and TerraSAR-X, they are optical satellites with multispectral sensors. Free public-domain satellite data can be a good choice for countries with limited budgets for airborne platforms. This section focuses on analyzing the impact of the three resolutions of satellite images on the accuracy of WBP early monitoring.

**4.5.1. Spatial resolution.** There are few studies comparing WBP monitoring accuracies among images with different spatial resolutions under the same conditions. At both the individual tree and stand levels, higher-resolution satellite data increase the accuracy of early monitoring of *D. valens* (133) and *I. typographus* (4, 5).

It is understandable that, at the early stages of a WBP infestation, only individual trees or clusters of trees are damaged. In coarse pixels, they are easily mixed with the background, shadows, understory, and overlapping tree canopies (14, 25, 99). Improving spatial resolution can reduce the

**Table 2 Commonly used satellites in WBP early detection studies**

| Satellite | Country or region | Temporal resolution (day) | Optical spectral resolution (nm) | Bands | Spatial resolution (m) | Is it free? | Case studies |
|---|---|---|---|---|---|---|---|
| Landsat 8 | United States | 16 | 20–60 (VNIR)<br>80–180 (SWIR)<br>600–1,000 (TIR) | Pan, MS (coastal, R, G, B, NIR, 2 SWIR, Cirrus), 2 TIR | Pan: 15; MS: 30; TIR: 100 | Yes | 3, 4, 33, 46, 126 |
| Worldview-2 | United States | 1.1 | 20–140 (VNIR)<br>40 (red edge)<br>80–180 (SWIR) | Pan, MS (coastal, B, G, R, 2 NIR, Y, red edge) | Pan: 0.5; MS: 2 | No | 55, 86–88, 143 |
| Quickbird | United States | 1–6 | 70–140 (VNIR) | Pan, MS (B, G, R, NIR) | Pan: 0.61; MS: 2.44 | No | 124 |
| Gaofen-2 | China | 5 | 70–120 (VNIR) | Pan, MS (B, G, R, NIR) | Pan: 0.8; MS: 3.2 | No | 133 |
| Sentinel-2 | Europe | 5 | 27–145 (VNIR)<br>18–19 (red edge)<br>75–243 (SWIR) | MS (coastal, B, G, R, 3 red edge, NIR, water vapor, SWIR-Cirrus, 2 SWIR) | B, G, R, NIR: 10; red edge, SWIR: 20; other: 60 | Yes | 4, 8, 29, 52, 133 |
| SPOT-5 | France | 26 | 90–100 (VNIR)<br>170 (SWIR) | Pan, MS (G, R, NIR, SWIR) | Pan: 2.5; MS: 10; SWIR: 20 | No | 5 |
| RapidEye | Germany | 5.5 | 55–90 (VNIR)<br>40 (red edge) | MS (B, G, R, red edge, NIR) | MS: 5 | No | 63, 93 |
| TerraSAR-X | Germany | 11 | NA | Radar, X band (wavelength: 3cm) | 1–40 | No | 93 |
| Sentinel-1 | Europe | 6 | NA | Radar, C band (wavelength: 6cm) | ≥5 | Yes | 52 |

Abbreviations: B, blue band; G, green band; MS, multispectral band; NIR, near-infrared band; Pan, panchromatic band; R, red band; SWIR, short-wave infrared band; TIR, thermal infrared; VNIR, visible and NIR.

mixed-pixel effects. Better results were obtained using images with pixel sizes of no more than an individual crown size (77, 121). Currently, many satellites used for WBP early monitoring, such as Landsat 8 and Sentinel-2, have insufficient spatial resolution to detect a single tree accurately.

Thus, the choice of satellites should take into account both spatial resolution and application purpose. To map the large-scale occurrence of WBPs, a spatial resolution of 15–100 m (such as that of Landsat and Sentinel-2) should be sufficient. A spatial resolution of 1–15 m (such as that of SPOT-5) is suitable for monitoring forest stands with few damaged trees. When analyzing individual trees, submeter-spatial-resolution sensors (such as Worldview-2 and Quickbird) are required to provide urgently needed calibration and validation data (123).

**4.5.2. Spectral resolution.** Spectral resolution refers to the number and bandwidth of spectral bands of a satellite sensor. The multispectral sensors listed in **Table 2** have relatively wide bandwidths. However, their number of spectral bands varies significantly, especially for the red edge and SWIR bands, which affects the monitoring accuracy.

The visible-light, red edge, NIR, and SWIR regions of the electromagnetic spectrum are generally used to monitor the changes in canopy water content, pigment content, and cell structure caused by WBPs (13, 27, 31, 33, 66). Blue to red edge bands play a very important role in WBP early monitoring (5, 8, 20, 27, 52, 143). Higher visible-light reflectances from damaged trees than from healthy ones have been found in infestation of *I. typographus* (5). Similar results have also been found with the red edge band to monitor early stage bark beetle damage (55, 86). In the NIR bands, healthy stands normally have higher reflectances than do damaged stands (33, 55, 87, 93). The SWIR region of the spectrum is also key for distinguishing healthy trees from those damaged

by *I. typographus* and *D. rufipennis* (5, 8, 33, 52). In addition, monitoring using SIF requires ultra-high spectral resolution (approximately 0.5 nm), which current satellite sensors cannot provide. Generally, the most-used bands from spaceborne sensors are, in order, NIR, red edge, and SWIR.

These bands have been used to generate a few stress-sensitive spectral indices (SIs) to assess the WBP infestation status, such as the Normalized Difference Vegetation Index (NDVI), Normalized Difference Red Edge Index (NDRE), Normalized Difference Moisture Index (NDMI), and Modified Simple Ratio (MSI) (4, 5, 8, 38, 34, 35, 52, 93, 106, 124, 126, 127). The accuracy of early monitoring using a vegetation index was found to be 71–86% for *D. ponderosae* (38) and 80–82% for *I. typographus* (52). The wetness index was also found to be promising for early detection of *I. typographus* (8, 40).

**Spectral indices (SIs):** a variety of indices obtained from spectral reflectance transformations

SIs provide an efficient method to utilize these bands. However, there are still two major issues to address in future WBP early monitoring using optical bands or spectral indices: (*a*) differentiation of the confounding effects of phenological change, climate change, and other stressors (e.g., diseases and other pests) (43, 79, 105, 106, 108) and (*b*) improvement of the portability or universality of the applied bands or indices.

**4.5.3. Temporal resolution.** The temporal resolution of satellite images, mainly determined by the revisit period, significantly impacts WBP early monitoring accuracy. The selection of suitable satellites and monitoring periods should include the flight period of the WBP.

Generally, the flight period varies across different WBP species. In China, *D. valens* begin to fly in late April and ends in mid-June (138), while *Monochamus alternatus* fly from late March to late June. Moreover, differences in climatic conditions among regions cause differences in the flight period of adult insects and different generations of insects. The flight period of *M. alternatus* varies between northern China (early May to late June) and southern China (late March to mid-June) (141). In Europe, *I. typographus* generally fly from April to May (2); however, the flight activity has extended from mid-April to mid-August in southern Sweden due to warming (92). Meanwhile, high temperatures from June to August allow two generations of *I. typographus* in Central Europe (89), increasing the flight time and frequency.

Time series of satellite data have not been fully utilized. In previous studies, a single-date image was often used to classify or quantitatively inverse WBP damage according to the differences in reflectance or SI (4, 15, 20, 71, 93, 121, 133, 143). Multitemporal images provide spatiotemporal information for dynamic monitoring and achieve higher accuracy (39, 64, 68, 85, 102, 127). The multidate method was more accurate in identifying *D. ponderosae*–damaged stands with light or moderate mortality (78). Multidate images also allow one to find the optimal observation period to identify the entire life cycle for better understanding of WBP occurrence, spread, and outbreaks (8, 52).

However, there are still issues to be addressed. First, some insects have several generations in a year, and their survival will be affected by climate and region. Therefore, the optimal observation period may change accordingly and must be adjusted regularly. Second, temporal resolution should not be determined alone because the spatial and spectral resolution, data quality, processing cost, and coverage area of satellite images all affect WBP early monitoring accuracy. Thus, it is important to find an effective method to jointly construct time-series data to derive comprehensive insights from multisource satellites.

## 4.6. Detection Models

Detection models transform RS data into WBP monitoring results. The quality of a detection model or classification algorithm directly determines the WBP monitoring accuracy. Most

**Table 3 Commonly used models or algorithms in WBP early detection studies**

| Algorithm | Input data distribution requirement | Training sample size | Universality | Algorithmic complexity | Case studies |
|---|---|---|---|---|---|
| Random forest | No | ▲ | ▲▲▲ | ▲ | 8, 33, 52, 57, 88, 131, 143 |
| Support vector machine | No | ▲ | ▲▲▲ | ▲▲ | 27, 129, 133, 143 |
| Classification and regression tree | No | ▲ | ▲▲▲ | ▲ | 38, 66, 133 |
| Discriminant analysis | Yes | ▲▲ | ▲▲ | ▲ | 31, 45, 59 |
| Linear regression | Yes | ▲▲ | ▲▲ | ▲ | 40, 52, 96 |
| Partial least squares regression | Yes | ▲▲ | ▲▲ | ▲▲ | 2 |
| Logistic regression | Yes | ▲▲ | ▲▲ | ▲ | 40 |
| Maximum likelihood classifiers | Yes | ▲▲ | ▲▲▲ | ▲▲ | 43, 61 |
| Convolutional neural network | No | ▲▲▲ | ▲▲ | ▲▲▲ | 122, 128, 129 |

▲ indicates extent. Abbreviation: WBP, wood-boring pest.

studies adopted supervised classification algorithms (**Table 3**), while very few studies were found to use unsupervised classification methods for WBP detection (121). Currently, two model types are used in the early monitoring of WBPs: parametric and nonparametric models. Parametric models have solid mathematical and statistical foundations to fit practical data and are easy to use. Linear regression, logistic regression, and partial least squares regression are widely used (2, 31, 40, 59, 71, 85, 96, 108, 109, 119). The linear regression model has been successfully used to evaluate the ability of LiDAR parameters to distinguish different damage levels of *I. typographus* through correlation with defoliation, discoloration, and resin flow (59). However, parametric models require that the input data conform to certain preconditions, like the homogeneity of variance, which may not always be feasible. As an alternative, nonparametric models such as random forest and support vector machine have little dependence on data distribution and types. These machine learning models are widely used in WBP monitoring research (8, 24, 52, 56, 60, 102, 105, 129–131, 143). As an advancement of machine learning, deep learning can automatically learn and extract richer and deeper features through deep networks than can traditional machine learning (7). Thus, the number of studies using deep learning algorithms in WBP monitoring has been rapidly increasing (60, 98, 125, 134). Most studies still focus on detecting WBP infestations in the late stage, while studies on early monitoring are relatively few (122, 128, 129). A deep learning model (3D convolutional neural network) was developed to simultaneously extract crown spectral and spatial information to identify early damaged trees infested by *B. xylophilus*, with a promising accuracy of 72.86% (128).

In short, most detection models used in WBP early monitoring are machine learning algorithms; parametric models are less used due to their prerequisites on data distribution and types; and, despite their more frequent application to late infestation stage detection in current studies, deep learning algorithms have great potential to detect the early stage of WBP infestation.

Furthermore, RS mechanism models can help machine learning algorithms to improve data quality, model universality, and result accuracy. The PROSPECT (19) and LIBERTY (28) models have been used for simulating leaf spectra from physiological parameters. Canopy reflectance simulation models such as stochastic radiative transfer (67), 4-Scale (18), and radiosity applicable to porous individual objects (RAPID) (48, 49) scale reflectance from the leaf to the entire canopy. Such scaling has improved detection accuracy of *Tomicus* spp. by providing prior knowledge and training data for machine learning models (67, 69, 71).

**Random forest:** a machine learning approach for image classification and regression analysis that grows and combines multiple decision trees to create a forest

**Support vector machine:** a machine learning approach for two-group classification problems

**Convolutional neural network:** a deep learning approach for image classification

**Stochastic radiative transfer:** a radiative transfer model applicable to simulating the radiation regime in forest canopies with horizontally distributed heterogeneity

## 5. KEY ISSUES AND TECHNOLOGIES

Some challenging problems exist in WBP early monitoring. Some of the major issues and possible solutions are discussed below.

**Radiosity applicable to porous individual objects (RAPID):** a 3D radiative transfer model that simulates a tree canopy as made up of porous individual objects

### 5.1. Identification of Host Tree Species

WBP monitoring is relatively easy in plantation forests due to their single host tree species. In mixed forests, the same WBP species often damages multiple hosts simultaneously. Therefore, a forest type or tree species map is required as background information to accurately locate host trees to help assess the damage situation, analyze occurrence dynamics, and predict WBP spread. However, such information is often lacking or outdated. Recent advances in RS technology can provide multisource data for tree species identification, such as visible light (12), NIR (117), TIR (74), multispectral (118), hyperspectral (135), and LiDAR (11) or SAR data (22), as well as data fusion (62).

While tree species classification based on RS data has become an important research topic, there are still several challenges. Studies have achieved high accuracy, but most studies classify tree species among different families and genera. However, for WBPs, most host tree species belong to the same family or even the same genus with high similarity (e.g., *Pinus massoniana* and *Pinus thunbergii*) and are very challenging to separate. Multisource RS data and multitemporal data can be used to replace single-source or single-date RS data to achieve refined and precise tree species maps.

The classification accuracy of tree species at the satellite scale needs to be improved. Dense time series of Sentinel-2 images were used to classify several dominant tree species in central Europe with an accuracy of 66.8–98.9%, but they showed lower accuracy for minor tree species (44). Sentinel-1 and Sentinel-2 data were combined to classify three hosts of *Choristoneura fumigerana*, resulting in an accuracy of approximately 72% (9). Worldview-3 and Pléiades were also explored for classifying single-tree species, with an accuracy of less than 90% (30, 97).

In such a situation, adding texture features of tree crowns may improve the classification accuracy of tree species, as these features can reflect the local spatial information related to image tone changes (11). However, texture features vary with seasons, climates, or soils. Therefore, if one is including texture characteristics, phenology should also be considered.

### 5.2. Type of Forest Disturbance

Forest disturbance is one of the major drivers of forest ecosystem changes (23, 41, 65, 94, 116). A forest may possibly be disturbed simultaneously or successively by multiple factors, such as various pests, drought, wind-fall, and harvest. A clear distinction among these factors is crucial for better understanding the occurrence area, damage process, and spread of pests.

Numerous studies have used RS technology to accurately distinguish pests from other abiotic forest disturbances such as wind-fall, fire, harvest, and lightning strikes (1, 17, 21, 83, 104, 105). A few studies have also distinguished forest pests and diseases of different damage types, like WBPs and defoliators (42, 79, 106). However, research on differentiating various WBPs that cause similar damage is lacking.

In China, *B. xylophilus* and *D. valens* often endanger the same tree species, such as *Pinus tabuliformis* and *Pinus sylvestris* var. *mongolica*. Changes in the color and texture of tree crowns shown in the RS images of trees damaged by these two pests are almost identical; thus, the effects of these pests are challenging to discriminate. Additionally, the host tree species harmed by the two pests have a high degree of overlap, mostly belonging to the genus *Pinus*. Thus, it is unrealistic to identify the two pests based on their hosts. Moreover, the occurrence time of both pests is almost

the same; thus, there is no solid basis to distinguish them based on time of occurrence. Reliable prior knowledge and a large amount of ground survey data are necessary to accurately distinguish them, but these are difficult to achieve on a large scale. Accordingly, we should establish a system to record the distribution of WBPs and their host tree species in each region or worldwide, with regular updates, and to provide a reliable reference for future research. The host tree species distribution, landscape patterns, phenology, and climate features should also be considered in addition to the color, shape, and texture characteristics of tree crowns (23, 105, 136).

### 5.3. Lack of Ground Truth

Ground truth data from independent site measurements are indispensable to build a WBP detection model for training or validation. The quantity and quality of ground truth data directly determine model generalization and accuracy. However, acquiring ground truth data is costly, especially for large-scale monitoring, leading to a lack of high-quality data.

The following approaches can be considered to compensate for this deficiency. Data augmentation can be used on UAV images as a surrogate for ground truth. Geometric transformations such as flipping, rotating, and deforming are generally performed on images to increase training samples and improve model generalization. Migration learning and generative adversarial networks are also powerful for data augmentation (36, 37, 139). Unsupervised classification, totally based on image feature space, is another choice that does not require training data. Simulating pest damage and RS canopy images through mechanistic models (such as RAPID) has become a meaningful way to provide sufficient training data. The representativeness of the training data also needs to increase, and sample distribution should be well balanced among categories. Common approaches for balancing samples include improvements to the sampling strategy, use of suitable weights, and use of prior knowledge (76, 90, 101). New data collection technologies, such as close-range RS, the internet of things, and big data technology, can also be introduced to obtain ground truth data efficiently.

#### SUMMARY POINTS

1. Hyperspectral RS is the most suitable approach for WBP early monitoring, and red edge, NIR, and SWIR are the most sensitive bands to monitor tree health status. However, operational hyperspectral satellites are urgently required.
2. More studies have been conducted, and higher accuracies have been demonstrated, using airborne sensors than using satellite sensors. However, satellite sensors allow monitoring at a variety of scales, from an individual tree (e.g., Worldview-2, QuickBird), to a stand (e.g., RapidEye, SPOT-5), to global forests (e.g., Landsat 8, Sentinel-2). A satellite spatial resolution comparable to an individual tree crown size is the best.
3. Early detection of WBP damage is scale dependent. Field sensors can detect a few red shoots or crowns, while airborne or spaceborne sensors can detect clusters of red crowns or possibly green crowns under stress using UAV hyperspectral signals. Thus, to our knowledge, the current early stage detection mostly occurs at the discoloring stage, but several studies show exciting results at the green stage.
4. There is an increasing interest in deep learning, and machine learning algorithms are the first choice for WBP early monitoring. Additionally, detection models fusing all kinds of RS data have also been proposed.

5. In addition to the color, shape, and texture characteristics of tree crowns, prior knowledge of host tree species distribution, characteristics of landscape patterns, phenology, and climate should also be considered.

### FUTURE ISSUES

1. Existing RS technology can monitor tree symptoms but cannot precisely identify WBP species. Thus, identifying a clear link between tree symptoms and WBP species requires further exploration, possibly by developing databases based on high-resolution mapping of tree species, the historical occurrence of WBP damage, and on-site continuous UAV observations.
2. More sensitive sensors are still required to detect tiny changes in tree morphological, physiological, and ecological characteristics in the early monitoring of WBPs. Chlorophyll fluorescence, which shows an excellent potential for use to monitor crop diseases and pests, needs to be tested.
3. There is a need for practical artificial intelligence detection models; such models should be simple, fast, stable, and accurate. Accordingly, sufficient training samples need to be generated when the ground truth data are insufficient.
4. To improve detection efficiency, countries should establish national early warning systems that integrate field, airborne, and spaceborne data and provide rapid estimates of forest disturbances, including WBP infestations.

## DISCLOSURE STATEMENT

The authors are not aware of any affiliations, memberships, funding, or financial holdings that might be perceived as affecting the objectivity of this review.

## AUTHOR CONTRIBUTIONS

Y.L. was responsible for conception of the idea and coordination; Y.L. and A.R. were responsible for information on wood-boring pests; and H.H. was responsible for information on remote sensing technology. All authors drafted the manuscript, commented on the manuscript, and approved the final version.

## ACKNOWLEDGMENTS

We thank Run Yu, Yujie Liu, and Linfeng Yu for data collection, statistics analysis, and chart making. We gratefully acknowledge Lili Ren for help with communication, coordination, and illustrations. This work was supported by the National Key R&D Program of China (grant 2021YFD1400900) and the Major Emergency Science and Technology Project of National Forestry and Grassland Administration (grant ZD202001). We apologize to the many authors whose work we were unable to highlight due to space limitations.

## LITERATURE CITED

1. Abdel-Rahman EM, Mutanga O, Adam E, Ismail R. 2014. Detecting *Sirex noctilio* grey-attacked and lightning-struck pine trees using airborne hyperspectral data, random forest and support vector machines classifiers. *ISPRS J. Photogramm. Remote Sens.* 88:48–59

2. Abdullah H, Darvishzadeh R, Skidmore AK, Groen TA, Heurich M. 2018. European spruce bark beetle (*Ips typographus*, L.) green attack affects foliar reflectance and biochemical properties. *Int. J. Appl. Earth Obs. Geoinf.* 64:199–209
3. Abdullah H, Darvishzadeh R, Skidmore AK, Heurich M. 2019. Sensitivity of Landsat-8 OLI and TIRS data to foliar properties of early stage bark beetle (*Ips typographus*, L.) infestation. *Remote Sens.* 11(4):398
4. Abdullah H, Skidmore AK, Darvishzadeh R, Heurich M. 2019. Sentinel-2 accurately maps green-attack stage of European spruce bark beetle (*Ips typographus*, L.) compared with Landsat-8. *Remote Sens. Ecol. Conserv.* 5(1):87–106
5. Abdullah H, Skidmore AK, Darvishzadeh R, Heurich M. 2019. Timing of red-edge and shortwave infrared reflectance critical for early stress detection induced by bark beetle (*Ips typographus*, L.) attack. *Int. J. Appl. Earth Obs. Geoinf.* 82:101900
6. Ahern FJ. 1988. The effects of bark beetle stress on the foliar spectral reflectance of lodgepole pine. *Int. J. Remote Sens.* 9(9):1451–68
7. Ba J, Caruana R. 2014. Do deep nets really need to be deep? In *Advances in Neural Information Processing Systems 27 (NIPS 2014)*, pp. 2654–62. N.p.: NeurIPS
8. Barta V, Lukes P, Homolova L. 2021. Early detection of bark beetle infestation in Norway spruce forests of Central Europe using Sentinel-2. *Int. J. Appl. Earth Obs. Geoinform.* 100:102335
9. Bhattarai R, Rahimzadeh-Bajgiran P, Weiskittel A, Meneghini A, MacLean DA. 2021. Spruce budworm tree host species distribution and abundance mapping using multi-temporal Sentinel-1 and Sentinel-2 satellite imagery. *ISPRS J. Photogramm. Remote Sens.* 172:28–40
10. Buddenbaum H, Rock G, Hill J, Werner W. 2015. Measuring stress reactions of beech seedlings with PRI, fluorescence, temperatures and emissivity from VNIR and thermal field imaging spectroscopy. *Eur. J. Remote Sens.* 48(1):263–82
11. Cao JJ, Leng WC, Liu K, Liu L, He Z, Zhu YH. 2018. Object-based mangrove species classification using unmanned aerial vehicle hyperspectral images and digital surface models. *Remote Sens.* 10(1):89
12. Chenari A, Erfanifard Y, Dehghani M, Pourghasemi HR. 2017. Woodland mapping at single-tree levels using object-oriented classification of unmanned aerial vehicle (UAV) images. *Int. Arch. Photogramm. Remote Sens. Spatial Inf. Sci.* XLII-4/W4:43–49
13. Cheng T, Rivard B, Sánchez-Azofeifa GA, Feng J, Calvo-Polanco M. 2010. Continuous wavelet analysis for the detection of green attack damage due to mountain pine beetle infestation. *Remote Sens. Environ.* 114:899–910
14. Cole B, McMorrow J, Evans M. 2014. Spectral monitoring of moorland plant phenology to identify a temporal window for hyperspectral remote sensing of peatland. *ISPRS J. Photogramm. Remote Sens.* 90:49–58
15. Coops NC, Johnson M, Wulder MA, White JC. 2006. Assessment of QuickBird high spatial resolution imagery to detect red attack damage due to mountain pine beetle infestation. *Remote Sens. Environ.* 103:67–80
16. Coops NC, Varhola A, Bater CW, Teti P, Boon S, et al. 2009. Assessing differences in tree and stand structure following beetle infestation using lidar data. *Can. J. Remote Sens.* 35(6):497–508
17. Coops NC, Wulder M, Iwanicka D. 2009. Large area monitoring with a MODIS-based Disturbance Index (DI) sensitive to annual and seasonal variations. *Remote Sens. Environ.* 113(6):1250–61
18. Croft H, Chen JM, Zhang Y, Simic A. 2013. Modelling leaf chlorophyll content in broadleaf and needle leaf canopies from ground, CASI, Landsat TM 5 and MERIS reflectance data. *Remote Sens. Environ.* 133:128–40
19. Dawson TP, Curran PJ, Plummer SE. 1998. LIBERTY: modeling the effects of leaf biochemical concentration on reflectance spectra. *Remote Sens. Environ.* 65(1):50–60
20. Dennison PE, Brunelle AR, Carter VA. 2010. Assessing canopy mortality during a mountain pine beetle outbreak using GeoEye-1 high spatial resolution satellite data. *Remote Sens. Environ.* 114:2431–35
21. Derose R, Long J, Ramsey R. 2011. Combining dendrochronological data and the disturbance index to assess Engelmann spruce mortality caused by a spruce beetle outbreak in southern Utah, USA. *Remote Sens. Environ.* 115(9):2342–49
22. Dickinson C, Siqueira P, Clewley D, Lucas R. 2013. Classification of forest composition using polarimetric decomposition in multiple landscapes. *Remote Sens. Environ.* 131:206–14

23. Edwards D, Tobias J, Sheil D, Meijaard E, Laurance W. 2014. Maintaining ecosystem function and services in logged tropical forests. *Trends Ecol. Evol.* 29(9):511–20
24. Einzmann K, Atzberger C, Pinnel N, Glas C, Bock S, et al. 2021. Early detection of spruce vitality loss with hyperspectral data: results of an experimental study in Bavaria, Germany. *Remote Sens. Environ.* 266:112676
25. Eriksson H, Eklundh L, Kuusk A, Nilson T. 2006. Impact of understory vegetation on forest canopy reflectance and remotely sensed LAI estimates. *Remote Sens. Environ.* 103:408–18
26. FAO. 2009. *Global review of forest pests and diseases*. FAO For. Pap. 156, Food Agric. Org. U. N., Rome
27. Fassnacht FE, Latifi H, Ghosh A, Joshi PK, Koch B. 2014. Assessing the potential of hyperspectral imagery to map bark beetle-induced tree mortality. *Remote Sens. Environ.* 140:533–48
28. Feret JB, François C, Asner GP, Gitelson AA, Martin RE, et al. 2011. PROSPECT-4 and 5: advances in the leaf optical properties model separating photosynthetic pigments. *Remote Sens. Environ.* 112(6):3030–43
29. Fernandez-Carrillo A, Patočka Z, Dobrovolný L, Franco-Nieto A, Revilla-Romero B. 2020. Monitoring bark beetle forest damage in central Europe: a remote sensing approach validated with field data. *Remote Sens.* 12(21):3634
30. Ferreira MP, Wagner FH, Aragão LEOC, Shimabukuro YE, de Souza Filho CR. 2019. Tree species classification in tropical forests using visible to shortwave infrared WorldView-3 images and texture analysis. *ISPRS J. Photogramm. Remote Sens.* 149:119–31
31. Finley K, Chhin S, Nzokou P, O'Brien J. 2016. Use of near-infrared spectroscopy as an indicator of emerald ash borer infestation in white ash stem tissue. *For. Ecol. Manag.* 366:41–52
32. Fisher JB, Lee B, Purdy AJ, Halverson GH, Dohlen MB, et al. 2020. ECOSTRESS: NASA's next generation mission to measure evapotranspiration from the international space station. *Water Resour. Res.* 56(4):e2019WR026058
33. Foster AC, Walter JA, Shugart HH, Sibold J, Negron J. 2017. Spectral evidence of early-stage spruce beetle infestation in Engelmann spruce. *For. Ecol. Manag.* 384:347–57
34. Gitelson AA, Kaufman YJ, Merzlyak MN. 1996. Use of a green channel in remote sensing of global vegetation from EOS-MODIS. *Remote Sens. Environ.* 58:289–98
35. Gitelson AA, Viña A, Ciganda V, Rundquist DC, Arkebauer TJ. 2005. Remote estimation of canopy chlorophyll content in crops. *Geophys. Res. Lett.* 32:L08403
36. Goodfellow I, Pouget-Abadie J, Mirza M, Xu B, Warde-Farley D, et al. 2014. Generative adversarial networks. arXiv:1406.2661 [stat.ML]
37. Goodfellow I, Pouget-Abadie J, Mirza M, Xu B, Warde-Farley D, et al. 2020. Generative adversarial networks. *Commun. ACM* 63:139–44
38. Goodwin NR, Coops NC, Wulder MA, Gillanders S, Schroeder TA, Nelson T. 2008. Estimation of insect infestation dynamics using a temporal sequence of Landsat data. *Remote Sens. Environ.* 112:3680–89
39. Goodwin NR, Magnussen S, Coops NC, Wulder MA. 2010. Curve fitting of time-series Landsat imagery for characterizing a mountain pine beetle infestation. *Int. J. Remote Sens.* 31:3263–71
40. Hais M, Wild J, Berec L, Brůna J, Kennedy R, et al. 2016. Landsat imagery spectral trajectories—important variables for spatially predicting the risks of bark beetle disturbance. *Remote Sens.* 8(8):687
41. Hansen WD, Chapin FS, Naughton HT, Rupp TS, Verbyla D. 2016. Forest-landscape structure mediates effects of a spruce bark beetle (*Dendroctonus rufipennis*) outbreak on subsequent likelihood of burning in Alaskan boreal forest. *For. Ecol. Manag.* 369:38–46
42. Hatala JA, Crabtree RL, Halligan KQ, Moorcroft PR. 2010. Landscape-scale patterns of forest pest and pathogen damage in the Greater Yellowstone Ecosystem. *Remote Sens. Environ.* 114(2):375–84
43. Havašová M, Ferenčík J, Jakuš R. 2017. Interactions between windthrow, bark beetles and forest management in the Tatra national parks. *For. Ecol. Manag.* 391:349–61
44. Hemmerling J, Pflugmacher D, Hostert P. 2021. Mapping temperate forest tree species using dense Sentinel-2 time series. *Remote Sens. Environ.* 267:112743

45. Hilker T, Coops NC, Coggins SB, Wulder MA, Brown M, et al. 2009. Detection of foliage conditions and disturbance from multi-angular high spectral resolution remote sensing. *Remote Sens. Environ.* 113:421–34
46. Host TK, Russell MB, Windmuller-Campione MA, Slesak RA, Knight JF. 2020. Ash presence and abundance derived from composite Landsat and Sentinel-2 time series and lidar surface models in Minnesota, USA. *Remote Sens.* 12(8):1341
47. Hu B, Li J, Wang J, Hall B. 2014. The early detection of the emerald ash borer (EAB) using advanced geospatial technologies. *Int. Arch. Photogramm. Remote Sens. Spatial Inf. Sci.* XL-2:213–19
48. Huang HG, Qin WH, Liu QH. 2013. RAPID: a radiosity applicable to porous individual objects for directional reflectance over complex vegetated scenes. *Remote Sens. Environ.* 132(10):221–37
49. Huang HG, Zhang ZY, Ni WJ, Chai L, Qin WH, et al. 2018. Extending RAPID model to simulate forest microwave backscattering. *Remote Sens. Environ.* 217(10):272–91
50. Huang K, Huang HG. 2019. Using ground-based LiDAR to detect shoot dieback: a case study on Yunnan pine shoots. *Remote Sens. Lett.* 10(7–9):903–12
51. Hunt ER, Rock BN. 1989. Detection of changes in leaf water content using near- and middle-infrared reflectance. *Remote Sens. Environ.* 30(1):43–54
52. Huo LN, Persson H J, Lindberg E. 2021. Early detection of forest stress from European spruce bark beetle attack, and a new vegetation index: normalized distance red & SWIR (NDRS). *Remote Sens. Environ.* 255:112240
53. Huo LN, Zhang N, Zhang XL, Wu YS. 2019. Tree defoliation classification based on point distribution features derived from single-scan terrestrial laser scanning data. *Ecol. Indic.* 103:782–90
54. Huo LN, Zhang XL. 2019. A new method of equiangular sectorial voxelization of single-scan terrestrial laser scanning data and its applications in forest defoliation estimation. *ISPRS J. Photogramm. Remote Sens.* 151:302–12
55. Immitzer M, Atzberger C. 2014. Early detection of bark beetle infestation in Norway spruce (*Picea abies*, L.) using WorldView-2. *Photogramm. Fernerkund.* 5:351–67
56. Iordache M-D, Mantas V, Baltazar E, Pauly K, Lewyckyj N. 2020. A machine learning approach to detecting pine wilt disease using airborne spectral imagery. *Remote Sens.* 12(14):2280
57. Ismail R, Mutanga O. 2011. Discriminating the early stages of *Sirex noctilio* infestation using classification tree ensembles and shortwave infrared bands. *Int. J. Remote Sens.* 32(15):4249–66
58. Jin RH, Zhang HM, Lin P. 1991. Discussion on remote sensing monitoring of biological disasters. *Remote Sens. Inf.* 3:35–37
59. Junttila S, Holopainen M, Vastaranta M, Lyytikäinen-Saarenmaa P, Kaartinen H, et al. 2019. The potential of dual-wavelength terrestrial Lidar in early detection of *Ips typographus* (L.) infestation—leaf water content as a proxy. *Remote Sens. Environ.* 231:111264
60. Kislov D, Korznikov K, Altman J, Vozmishcheva A, Krestov P. 2021. Extending deep learning approaches for forest disturbance segmentation on very high-resolution satellite images. *Remote Sens. Ecol. Conserv.* 7:355–68
61. Klouček T, Komárek J, Surový P, Hrach K, Janata P, Vašíček B. 2019. The use of UAV mounted sensors for precise detection of bark beetle infestation. *Remote Sens.* 11(13):1561
62. Krzystek P, Serebryanyk A, Schnörr C, Červenka J, Heurich M. 2021. Large-scale mapping of tree species and dead trees in Šumava National Park and Bavarian Forest National Park using lidar and multispectral imagery. *Remote Sens.* 12(4):661
63. Latifi H, Dahms T, Beudert B, Heurich M, Kübert C, Dech S. 2018. Synthetic RapidEye data used for the detection of area-based spruce tree mortality induced by bark beetles. *GISci. Remote Sens.* 55(6):839–59
64. Latifi H, Fassnacht FE, Schumann B, Dech S. 2014. Object-based extraction of bark beetle (*Ips typographus* L.) infestations using multi-date Landsat and SPOT satellite imagery. *Prog. Phys. Geogr.* 38:755–85
65. Lausch A, Heurich M, Fahse L. 2013. Spatio-temporal infestation patterns of *Ips typographus* (L.) in the Bavarian Forest National Park, Germany. *Ecol. Indic.* 31:73–81
66. Lausch A, Heurich M, Gordalla D, Dobner H-J, Gwillym-Margianto S, Salbach C. 2013. Forecasting potential bark beetle outbreaks based on spruce forest vitality using hyperspectral remote-sensing techniques at different scales. *For. Ecol. Manag.* 308:76–89

67. Li XY, Huang HG, Nikolay V, Chen L, Yan K, Shi J. 2020. Extending the stochastic radiative transfer theory to simulate BRF over forests with heterogeneous distribution of damaged foliage inside of tree crowns. *Remote Sens. Environ.* 250:112040
68. Liang L, Chen YL, Hawbaker TJ, Zhu ZL, Gong P. 2014. Mapping mountain pine beetle mortality through growth trend analysis of time-series Landsat data. *Remote Sens.* 6(6):5696–716
69. Lin QN, Huang HG, Chen L, Wang J, Huang K, Liu Y. 2021. Using the 3D model RAPID to invert the shoot dieback ratio of vertically heterogeneous Yunnan pine forests to detect beetle damage. *Remote Sens. Environ.* 260(6):112475
70. Lin QN, Huang HG, Wang JX, Huang K, Liu YY. 2019. Detection of pine shoot beetle (PSB) stress on pine forests at individual tree level using UAV-based hyperspectral imagery and lidar. *Remote Sens.* 11(21):2540
71. Lin QN, Huang HG, Yu LF, Wang JX. 2018. Detection of shoot beetle stress on Yunnan pine forest using a coupled LIBERTY2-INFORM simulation. *Remote Sens.* 10(7):1133
72. Liu YJ, Zhan ZY, Ren LL, Ze SZ, Yu LF, et al. 2021. Hyperspectral evidence of early-stage pine shoot beetle attack in Yunnan pine. *For. Ecol. Manag.* 497:119505
73. Luo YQ, Liu YJ, Huang HG, Yu LF, Ren LL. 2021. Pathway and method of forest health assessment using remote sensing technology. *J. Beijing For. Univ.* 43(9):1–13
74. Luz B, Crowley JK. 2010. Identification of plant species by using high spatial and spectral resolution thermal infrared (8.0–13.5 μm) imagery. *Remote Sens. Environ.* 114(2):404–13
75. Majdák A, Jakuš R, Blaženec M. 2021. Determination of differences in temperature regimes on healthy and bark-beetle colonized spruce trees using a handheld thermal camera. *iForest* 14(3):203–11
76. Maltamo M, Bollandsas OM, Næsset E, Gobakken T, Packalén P. 2011. Different plot selection strategies for field training data in ALS-assisted forest inventory. *Forestry* 84:23–31
77. Meddens AJH, Hicke JA, Vierling LA. 2011. Evaluating the potential of multispectral imagery to map multiple stages of tree mortality. *Remote Sens. Environ.* 115:1632–42
78. Meddens AJH, Hicke JA, Vierling LA, Hudak AT. 2013. Evaluating methods to detect bark beetle-caused tree mortality using single-date and multi-date Landsat imagery. *Remote Sens. Environ.* 132:49–58
79. Meigs GW, Kennedy RE, Gray AN, Gregory MJ. 2015. Spatiotemporal dynamics of recent mountain pine beetle and western spruce budworm outbreaks across the Pacific Northwest Region, U.S.A. *For. Ecol. Manag.* 339:71–86
80. Meng R, Dennison PE, Zhao F, Shendryk L, Rickert A, et al. 2018. Mapping canopy defoliation by herbivorous insects at the individual tree level using bi-temporal airborne imaging spectroscopy and LiDAR measurements. *Remote Sens. Environ.* 215:170–83
81. Meroni M, Busetto L, Colombo R, Guanter L, Moreno J, Verhoef W. 2010. Performance of spectral fitting methods for vegetation fluorescence quantification. *Remote Sens. Environ.* 114(2):363–74
82. Meroni M, Colombo R. 2006. Leaf level detection of solar induced chlorophyll fluorescence by means of a subnanometer resolution spectroradiometer. *Remote Sens. Environ.* 103(4):438–48
83. Mildrexler D, Zhao M, Heinsch F, Running S. 2007. A new satellite-based methodology for continental-scale disturbance detection. *Ecol. Appl.* 17(1):235–50
84. Mohammed GH, Colombo R, Middleton EM, Rascher U, van der Tol C, et al. 2019. Remote sensing of solar-induced chlorophyll fluorescence (SIF) in vegetation: 50 years of progress. *Remote Sens. Environ.* 231:111177
85. Moisen GG, Meyer MC, Schroeder TA, Liao X, Schleeweis KG, et al. 2016. Shape selection in Landsat time series: a tool for monitoring forest dynamics. *Glob. Change Biol.* 22:3518–28
86. Mullen KE. 2016. *Early detection of mountain pine beetle damage in Ponderosa pine forests of the Black Hills using hyperspectral and WorldView-2 data*. MA Thesis, Minn. State Univ., Mankato
87. Mullen KE, Yuan F, Mitchell M. 2018. The mountain pine beetle epidemic in the Black Hills, South Dakota: the consequences of long-term fire policy, climate change and the use of remote sensing to enhance mitigation. *J. Geogr. Geol.* 10(1):69
88. Murfitt J, He Y, Yang J, Mui A, De Mille K. 2016. Ash decline assessment in emerald ash borer infested natural forests using high spatial resolution images. *Remote Sens.* 8(3):256
89. Netherer S, Panassiti B, Pennerstorfer J, Matthews B. 2019. Acute drought is an important driver of bark beetle infestation in Austrian Norway spruce stands. *Front. For. Glob. Chang.* 2:39

90. Nguyen HM, Begüm D, Dalponte M. 2019. A weighted SVM-based approach to tree species classification at individual tree crown level using LiDAR data. *Remote Sens.* 11(24):2948
91. Nowak DJ, Pasek JE, Sequeira RA, Crane DE, Mastro VC. 2001. Potential effect of *Anoplophora glabripennis* (Coleoptera: Cerambycidae) on urban trees in the United States. *J. Econ. Entomol.* 94(1):116–22
92. Öhrn P, Långström B, Lindelöw Å, Björklund N. 2014. Seasonal flight patterns of *Ips typographus* in southern Sweden and thermal sums required for emergence. *Agric. For. Entomol.* 16:147–57
93. Ortiz SM, Breidenbach J, Kändler G. 2013. Early detection of bark beetle green attack using TerraSAR-X and RapidEye data. *Remote Sens.* 5(4):1912–31
94. Pflugmachera D, Cohenb W, Kennedy R. 2012. Using Landsat-derived disturbance history (1972–2010) to predict current forest structure. *Remote Sens. Environ.* 122:146–65
95. Pontius J, Hanavan RP, Hallett RA, Cook BD, Corp LA. 2017. High spatial resolution spectral unmixing for mapping ash species across a complex urban environment. *Remote Sens. Environ.* 199:360–69
96. Pontius J, Martin M, Plourde L, Hallett R. 2008. Ash decline assessment in emerald ash borer-infested regions: a test of tree-level, hyperspectral technologies. *Remote Sens. Environ.* 112(5):2665–76
97. Pu R, Landry S. 2020. Mapping urban tree species by integrating multi-seasonal high resolution Pléiades satellite imagery with airborne LiDAR data. *Urban For. Urban Green.* 53:126675
98. Qin J, Wang B, Wu YL, Lu Q, Zhu HC. 2021. Identifying pine wood nematode disease using UAV images and deep learning algorithms. *Remote Sens.* 13(2):162
99. Rautiainen M, Lukeš P. 2015. Spectral contribution of understory to forest reflectance in a boreal site: an analysis of EO-1 Hyperion data. *Remote Sens. Environ.* 171:98–104
100. Rencz AN, Nemeth J. 1985. Detection of mountain pine beetle infestation using Landsat MSS and simulated thematic mapper data. *Can. J. Remote Sens.* 11(1):50–58
101. Roberge C, Wulff S, Reese H, Stähl G. 2016. Improving the precision of sample-based forest damage inventories through two-phase sampling and post-stratification using remotely sensed auxiliary information. *Environ. Monit. Assess.* 188:213
102. Rodman KC, Andrus RA, Butkiewicz CL, Chapman TB, Gill NS, et al. 2021. Effects of bark beetle outbreaks on forest landscape pattern in the southern Rocky Mountains, U.S.A. *Remote Sens.* 13(6):1089
103. Scherrer D, Bader KF, Körnera C. 2011. Drought-sensitivity ranking of deciduous tree species based on thermal imaging of forest canopies. *Agric. For. Meteorol.* 151(12):1632–40
104. Schroeder T, Wulder M, Healey S, Moisen GG. 2011. Mapping wildfire and clearcut harvest disturbances in boreal forests with Landsat time series data. *Remote Sens. Environ.* 115(6):1421–33
105. Sebald J, Senf C, Seidl R. 2021. Human or natural? Landscape context improves the attribution of forest disturbances mapped from Landsat in Central Europe. *Remote Sens. Environ.* 262(2):112502
106. Senf C, Pflugmacher D, Wulder MA, Hostert P. 2015. Characterizing spectral–temporal patterns of defoliator and bark beetle disturbances using Landsat time series. *Remote Sens. Environ.* 170:166–77
107. Senf C, Seidl R, Hostert P. 2017. Remote sensing of forest insect disturbances: current state and future directions. *Int. J. Appl. Earth Obs. Geoinform.* 60:49–60
108. Shen Q, Deng J, Liu XS, Huang HG. 2018. Prediction of bark beetles pests based on temperature vegetation dryness index. *Trans. Chin. Soc. Agric. Eng.* 34(9):167–74
109. Smigaj M, Gaulton R, Suárez JC, Barr SL. 2019. Canopy temperature from an Unmanned Aerial Vehicle as an indicator of tree stress associated with red band needle blight severity. *For. Ecol. Manag.* 433:699–708
110. Solberg S, Næsset E, Hanssen KH, Christiansen E. 2006. Mapping defoliation during a severe insect attack on Scots pine using airborne laser scanning. *Remote Sens. Environ.* 102:364–76
111. Song L, Guanter L, Guan KY, You LZ, Huete A, et al. 2018. Satellite sun-induced chlorophyll fluorescence detects early response of winter wheat to heat stress in the Indian Indo-Gangetic Plains. *Glob. Change Biol.* 24(9): 4023–37
112. Stereńczak K, Kraszewski B, Mielcarek M, Piasecka Ż. 2017. Inventory of standing dead trees in the surroundings of communication routes—the contribution of remote sensing to potential risk assessments. *For. Ecol. Manag.* 402:76–91
113. Stereńczak K, Mielcarek M, Modzelewska A, Kraszewski B, Fassnacht FE, Hilszczański J. 2019. Intra-annual *Ips typographus* outbreak monitoring using a multi-temporal GIS analysis based on hyperspectral and ALS data in the Białowieża Forests. *For. Ecol. Manag.* 442:105–16

114. Stone C, Mohammed C. 2017. Application of remote sensing technologies for assessing planted forests damaged by insect pests and fungal pathogens: a review. *Curr. For. Rep.* 3(2):75–92
115. Syifa M, Park SJ, Lee CW. 2020. Detection of the pine wilt disease tree candidates for drone remote sensing using artificial intelligence techniques. *Engineering* 6(8):919–26
116. Tanase MA, Aponte C, Mermoz S, Bouvet A, Le Toan T, Heurich M. 2018. Detection of windthrows and insect outbreaks by L-band SAR: a case study in the Bavarian Forest National Park. *Remote Sens. Environ.* 209:700–11
117. Ullah S, Schlerf M, Sikdmore A, Hecker C. 2012. Identifying plant species using mid-wave infrared (2.5–6 μm) and thermal infrared (8–14 μm) emissivity spectra. *Remote Sens. Environ.* 118:95–102
118. Valderrama-Landeros L, Flores-De-Santiago F, Kovacs JM, Flores-Verdugo F. 2018. An assessment of commonly employed satellite-based remote sensors for mapping mangrove species in Mexico using an NDVI-based classification scheme. *Environ. Monit. Assess.* 190(23):23
119. Vorster AG, Evangelista PH, Stohlgren TJ, Kumar S, Rhoades CC, et al. 2017. Severity of a mountain pine beetle outbreak across a range of stand conditions in Fraser Experimental Forest, Colorado, United States. *For. Ecol. Manag.* 389:116–26
120. Wang JX, Huang HG, Lin QN, Wang B, Huang K. 2019. Shoot beetle damage to *Pinus yunnanensis* monitored by infrared thermal imaging at needle scale. *Chin. J. Plant Ecol.* 43:959–68
121. White JC, Wulder MA, Brooks D, Reich R, Wheate R. 2005. Detection of red attack stage mountain pine beetle infestation with high spatial resolution satellite imagery. *Remote Sens. Environ.* 96:340–51
122. Wu BZ, Liang AJ, Zhang HF, Zhu T, Zou Z, et al. 2021. Application of conventional UAV-based high-throughput object detection to the early diagnosis of pine wilt disease by deep learning. *For. Ecol. Manag.* 486(2):118986
123. Wulder MA, White JC, Coggins SB, Ortlepp SM, Coops NC, et al. 2012. Digital high spatial resolution aerial imagery to support forest health monitoring: the mountain pine beetle context. *J. Appl. Remote Sens.* 6:06257
124. Wulder MA, White JC, Coops NC, Butson CR. 2008. Multi-temporal analysis of high spatial resolution imagery for disturbance monitoring. *Remote Sens. Environ.* 112:2729–40
125. Xia L, Zhang RR, Chen LP, Li LL, Yi TC, et al. 2021. Evaluation of deep learning segmentation models for detection of pine wilt disease in unmanned aerial vehicle images. *Remote Sens.* 13(18):3594
126. Ye S, Rogan J, Zhu Z, Hawbaker TJ, Hart SJ, et al. 2021. Detecting subtle change from dense Landsat time series: case studies of mountain pine beetle and spruce beetle disturbance. *Remote Sens. Environ.* 263(5):112560
127. Yu LF, Huang JX, Zong SX, Huang HG, Luo YQ. 2018. Detecting shoot beetle damage on Yunnan pine using Landsat time-series data. *Forests* 9(1):39
128. Yu R, Luo YQ, Li HN, Yang LF, Huang HG, et al. 2021. Three-dimensional convolutional neural network model for early detection of pine wilt disease using UAV-based hyperspectral images. *Remote Sens.* 13(20):4065
129. Yu R, Luo YQ, Zhou Q, Zhang XD, Ren LL. 2021. Early detection of pine wilt disease using deep learning algorithms and UAV-based multispectral imagery. *For. Ecol. Manag.* 497(4):119493
130. Yu R, Luo YQ, Zhou Q, Zhang XD, Wu DW, Ren LL. 2021. A machine learning algorithm to detect pine wilt disease using UAV-based hyperspectral imagery and LiDAR data at the tree level. *Int. J. Appl. Earth Obs. Geoinf.* 101(1):102363
131. Yu R, Ren LL, Luo YQ. 2021. Early detection of pine wilt disease in *Pinus tabuliformis* in North China using a field portable spectrometer and UAV-based hyperspectral imagery. *For. Ecosyst.* 8(3):583–601
132. Zarco-Tejada PJ, Camino C, Beck PSA, Calderon R, Hornero A, et al. 2018. Previsual symptoms of *Xylella fastidiosa* infection revealed in spectral plant-trait alterations. *Nat. Plants* 4(7):432–39
133. Zhan ZY, Yu LF, Li Z, Ren LL, Gao BT, et al. 2020. Combining GF-2 and Sentinel-2 images to detect tree mortality caused by red turpentine beetle during the early outbreak stage in North China. *Forests* 11(2):172
134. Zhang B, Ye HC, Lu W, Huang WJ, Wu B, et al. 2021. A spatiotemporal change detection method for monitoring pine wilt disease in a complex landscape using high-resolution remote sensing imagery. *Remote Sens.* 13(11):2083

135. Zhang B, Zhao L, Zhang XL. 2020. Three-dimensional convolutional neural network model for tree species classification using airborne hyperspectral images. *Remote Sens. Environ.* 247:111938
136. Zhang JG, Han HQ, Hu CH, Luo YQ. 2018. Identification method of *Pinus yunnanensis* pest area based on UAV multispectral images. *Trans. Chin. Soc. Agric. Mach.* 49(5):249–55
137. Zhang KW, Hu BX, Robinson J. 2014. Early detection of emerald ash borer infestation using multisourced data: a case study in the town of Oakville, Ontario, Canada. *J. Appl. Remote Sens.* 8(1):083602
138. Zhang LY, Chen QC, Zhang XB. 2002. Studies on the morphological characters and bionomics of *Dendroctonus valens* Leconte. *Sci. Silv. Sin.* 38(4):95–99
139. Zhang M, Gong M, He H, Zhu S. 2020. Symmetric all convolutional neural-network-based unsupervised feature extraction for hyperspectral images classification. *IEEE Trans. Cybern.* 52(5):2981–93
140. Zhang N, Zhang XL, Yang GJ, Zhu CH, Huo LN, Feng HK. 2018. Assessment of defoliation during the *Dendrolimus tabulaeformis* Tsai et Liu disaster outbreak using UAV-based hyperspectral images. *Remote Sens. Environ.* 217:323–39
141. Zhao YX, Dong Y, Xu ZH. 2004. Bionomics and geographical distribution of *Monochamus alternatus* Hope (Coleoptera: Cerambycidae) in Yunnan Province. *For. Pest Dis.* 23(5):13–16
142. Zhou K, Cao L. 2021. The status and prospects of remote sensing applications in precision silviculture. *Nat. Remote Sens. Bull.* 25(1):423–38
143. Zhou Q, Zhang XD, Yu LF, Ren LL, Luo YQ. 2021. Combining WV-2 images and tree physiological factors to detect damage stages of *Populus gansuensis* by Asian longhorned beetle (*Anoplophora glabripennis*) at the tree level. *For. Ecosyst.* 8:35